Journal of Neuroinflammation

RESEARCH Open Access

# ATP-evoked intracellular $Ca^{2+}$ transients shape the ionic permeability of human microglia from epileptic temporal cortex

Nicole Piera Palomba[1], Katiuscia Martinello[1*], Germana Cocozza[1], Sara Casciato[1], Addolorata Mascia[1], Giancarlo Di Gennaro[1], Roberta Morace[1], Vincenzo Esposito[1,2], Heike Wulff[3], Cristina Limatola[1,4] and Sergio Fucile[1,4]

## Abstract

**Background:** Intracellular $Ca^{2+}$ modulates several microglial activities, such as proliferation, migration, phagocytosis, and inflammatory mediator secretion. Extracellular ATP, the levels of which significantly change during epileptic seizures, activates specific receptors leading to an increase of intracellular free $Ca^{2+}$ concentration ($[Ca^{2+}]_i$). Here, we aimed to functionally characterize human microglia obtained from cortices of subjects with temporal lobe epilepsy, focusing on the $Ca^{2+}$-mediated response triggered by purinergic signaling.

**Methods:** Fura-2 based fluorescence microscopy was used to measure $[Ca^{2+}]_i$ in primary cultures of human microglial cells obtained from surgical specimens. The perforated patch-clamp technique, which preserves the cytoplasmic milieu, was used to measure ATP-evoked $Ca^{2+}$-dependent whole-cell currents.

**Results:** In human microglia extracellular ATP evoked $[Ca^{2+}]_i$ increases depend on $Ca^{2+}$ entry from the extracellular space and on $Ca^{2+}$ mobilization from intracellular compartments. Extracellular ATP also induced a transient fivefold potentiation of the total transmembrane current, which was completely abolished when $[Ca^{2+}]_i$ increases were prevented by removing external $Ca^{2+}$ and using an intracellular $Ca^{2+}$ chelator. TRAM-34, a selective $K_{Ca}3.1$ blocker, significantly reduced the ATP-induced current potentiation but did not abolish it. The removal of external $Cl^-$ in the presence of TRAM-34 further lowered the ATP-evoked effect. A direct comparison between the ATP-evoked mean current potentiation and mean $Ca^{2+}$ transient amplitude revealed a linear correlation. Treatment of microglial cells with LPS for 48 h did not prevent the ATP-induced $Ca^{2+}$ mobilization but completely abolished the ATP-mediated current potentiation. The absence of the $Ca^{2+}$-evoked $K^+$ current led to a less sustained ATP-evoked $Ca^{2+}$ entry, as shown by the faster $Ca^{2+}$ transient kinetics observed in LPS-treated microglia.

**Conclusions:** Our study confirms a functional role for $K_{Ca}3.1$ channels in human microglia, linking ATP-evoked $Ca^{2+}$ transients to changes in membrane conductance, with an inflammation-dependent mechanism, and suggests that during brain inflammation the $K_{Ca}3.1$-mediated microglial response to purinergic signaling may be reduced.

**Keywords:** Temporal lobe epilepsy, $K_{Ca}3.1$, Neuroinflammation, Purinergic signaling, Primary cultures, Perforated patch

* Correspondence: katiuscia.martinello@neuromed.it
[1]IRCCS Neuromed, Pozzilli, IS, Italy
Full list of author information is available at the end of the article

## Introduction

Epilepsy is a neurological disorder characterized by an altered balance between neuronal excitation and inhibition, involving profound changes in the function of brain networks and cells, including microglia [1]. Microglia are the resident immune cells of the central nervous system (CNS), where they play a homeostatic role of surveillance [2], contributing to synaptic pruning and neuromodulation [3, 4]. These key functions are regulated by the interaction of microglia with several modulatory molecules, including neurotransmitters, neuropeptides, and cytokines [5–7]. An important modulator of microglial functions is extracellular ATP [8], which is significantly altered during epileptic seizures [9]. Extracellular ATP activates specific ionotropic and metabotropic purinergic receptors on the microglial membrane, leading to an increase of intracellular free $Ca^{2+}$ concentration ($[Ca^{2+}]_i$) [10]. $Ca^{2+}$ is a key transducer modulating several microglial activities, such as proliferation, migration, phagocytosis, and inflammatory mediator secretion [11, 12]. In particular, changes in $[Ca^{2+}]_i$ rapidly tune the membrane ionic conductance [13] which, in turn, modulates relevant microglial function, such as motility, phagocytosis, and generation of ROS and cytokines [14]. Given that $Ca^{2+}$ activates membrane channels mainly through the interaction with diffusible mediators, such as cGMP [15], possible problems arise from the washout of crucial cytoplasmic diffusible factors in the usual conditions of whole-cell recordings [16, 17]. To avoid the loss of intracellular mediators of $Ca^{2+}$ activity, we here applied the perforated patch-clamp technique to the quantitative analysis of the ionic conductance induced by ATP-evoked $Ca^{2+}$ transients in human microglia isolated from the temporal cerebral cortices of adult epileptic patients. We identified the specific channels involved in the response to $[Ca^{2+}]_i$ increase before and after stimulation with LPS and confirmed a primary role for the intermediate-conductance $Ca^{2+}$-activated $K_{Ca}3.1$ channel [18, 19].

Our results are discussed in light of the modulation of $K_{Ca}3.1$ activity as a tool to modulate microglia-induced neuroinflammation in epileptic patients [20].

## Methods

### Patients

Surgical specimens were obtained from the temporal neocortex of 13 subjects with drug-resistant temporal lobe epilepsy (Table S1) operated on at the Epilepsy Surgery Center of IRCCS Neuromed, Pozzilli (IS), Italy. Informed consent was obtained from each patient to use part of the surgically resected material for experiments, and the local ethics committee approved the selection processes and procedures (approval number 5/2019).

### Isolation of primary human microglia

The isolation procedure was as described by Rustenhoven et al. [21]. Following surgical resection, tissue was transported to the research facility in cold HBSS in less than 20 min. Approximately 1-2 g of tissue was washed in HBSS (Gibco), and meninges and visible blood vessels were removed. Tissue was diced into pieces approximately 1 $mm^3$ using a sterile scalpel and transferred to a 50-mL falcon tube containing 10 mL enzyme dissociation mix (10 U/mL DNase (Invitrogen) and 2.5 U/mL papain (Worthington) in Hibernate-A medium (Gibco)) per gram of tissue for 10 min in an incubator at 37 °C with gentle rotation. The tissue was then gently triturated and returned to the incubator for another 10 min. Dissociation was slowed by adding an equal volume of Dulbecco's modified eagle medium: Nutrient mixture F-12 (DMEM/F12 with 1% FBS (Gibco). The cell suspension was passed through a 70 μm cell strainer (Becton Dickinson) to enhance culture homogeneity. Cells were centrifuged at 160×*g* for 10 min and resuspended in 20 mL of media containing DMEM/F12 with 1% FBS, 1% GlutaMAX (Gibco), 1% penicillin-streptomycin-glutamine (PSG). The cell suspension was transferred to Petri dishes and incubated overnight at 37 °C with 95% air/5% $CO_2$. The following day non-adherent or loosely adherent cells were removed. The adherent cells were washed twice, and culture media were added (DMEM/F12 with 10% FBS and 1% PSG). Cells were used for functional studies after at least 5 days in culture. Human microglial cells were activated by adding LPS (100 ng/ml) to the culture medium 48 h before the experiments [22, 23].

### Immunocytochemistry

Cells were fixed in 4% paraformaldehyde (ChemCruz) for 15 min and washed in PBS. After cell permeabilization with 0.2% Triton X-in PBS, cells were blocked (1% BSA in PBS) for 1 h, at RT, and incubated overnight at 4 °C with Iba1 and GFAP antibody (1:700; Wako) diluted in PBS with 0.1% BSA. Cells were washed three times in PBS and incubated with the fluorophore-conjugated secondary antibodies (1:2000, Catalog#A11012, A-21202, Invitrogen) for 45 min. After three washes in PBS, nuclei were counterstained with Hoechst 33258 for 5 min and cells washed in PBS. Coverslips were mounted on dishes using the Fluorescent Mounting Medium (DakoCytomation). Images were digitized using a CoolSNAP camera (Photometrics) coupled to an ECLIPSE Ti-S microscope (Nikon) and processed using MetaMorph 7.6.5.0 image analysis software (Molecular Device).

### Patch-clamp experiments

Currents were recorded with a Multiclamp 700B amplifier and Clampex 10.5 software (Molecular Devices) in

the perforated patch-clamp configuration to reduce the perturbation of the intracellular milieu, by using escin (50 μM). Patch-clamp recordings were obtained using borosilicate glass electrodes (4-6 MΩ) filled with different intracellular solutions: in the perforated patch or normal whole-cell configuration, in mM, K-gluconate 140, HEPES 10, BAPTA 5, $MgCl_2$ 2, and Mg-ATP 2, pH 7.3, adjusted with KOH; in normal whole-cell configuration, with 1 μM intracellular $Ca^{2+}$, in mM, K-gluconate 145, HEPES 10, EGTA 10, $CaCl_2$ 8.5, $MgCl_2$ 2, pH 7.3, adjusted with KOH. During recordings, cells were continuously perfused using normal external solutions (NES), containing, in mM, NaCl 140, HEPES 10, KCl 2.8, $CaCl_2$ 2, $MgCl_2$ 2, glucose 10, pH 7.3 adjusted with NaOH. In some experiments a low $Cl^-$ external solution was used, containing, in mM, Na-gluconate 140, HEPES 10, KCl 2.8, $CaCl_2$ 2, $MgCl_2$ 2, glucose 10. Cells were held at −70 mV and currents were elicited with voltage ramps (from −120 mV to +40 mV, 200 ms) every 2 s. The current density at −20 mV was determined as the current amplitude/cell capacitance (pA/pF). Cell capacitance was continuously monitored. To avoid $Ca^{2+}$ entry in the intracellular compartment, in selected experiments, a $Ca^{2+}$-free external solution was used, containing, in mM, NaCl 140, HEPES 10, KCl 2.8, EGTA 2, $MgCl_2$ 4, and glucose 10 (pH=7.3).

### $Ca^{2+}$-transient recordings

Changes in free intracellular $Ca^{2+}$ concentration ($[Ca^{2+}]_i$) were measured by time-resolved digital fluorescence microscopy, using an integrated acquisition system (Scientifica), composed of an upright reflected fluorescence microscope (Olympus) and the Optofluor software (Molecular Devices). Cells were incubated with the $Ca^{2+}$ indicator Fura-2 acetoxylmethylester (1 μM) for 45 min at 37 °C in culture medium. The changes of $[Ca^{2+}]_i$ were expressed as R = F340/F380, where F340 and F380 are the fluorescence intensities measured from individual cells at an emission wavelength of 510 nm illuminating the specimen with 340 and 380 nm excitation wavelengths, respectively. Cells were continuously perfused during the experiment. The acquisition frequency was 0.33 Hz.

### Data and statistical analysis

Data sampling was performed using the pClamp 10 software (Molecular devices) and the OptoFluor (CAIRN) software. Data analysis was performed using SigmaPlot 14.0 (Systat). All data are expressed as means ± standard error mean and analyzed using paired *t* test or one-way ANOVA, as appropriate. Significance for all tests was set at $p < 0.05$, with statistical power > 0.8. For each experiment, data were pooled from microglial cells obtained from the patients indicated in the corresponding figure legends. The linear regression is calculated by the SigmaPlot software by the least-squares method.

## Results

Human microglial cells play an important role in controlling the inflammatory status of the brain in epileptic patients [1]. To better define their functional role, we aimed to describe the molecular pathways activated in human microglia by activity-driven mechanisms, such as purinergic signaling [9, 24]. Thus, we established primary cultures of human microglia derived from the temporal cortex surgically resected from patients with temporal lobe epilepsy. These cultures were 98.8±1.2 % positive for Iba1 (Fig. 1a, b; *n*=7). The residual cells were contaminating astrocytes, as identified by GFAP staining (Fig. 1b). First, to study the functional relationship between $Ca^{2+}$ mobilization and the modulation of membrane conductance in human microglia, we quantified the $Ca^{2+}$ signaling elicited upon ATP stimulation [8]. We chose an extracellular ATP concentration of 100 μM based on two considerations: (i) the concentration should be able to elicit clear $Ca^{2+}$ transients in microglia [25]; (ii) the increase of ATP concentration is limited during seizures [24] and never reaches the millimolar range necessary to activate P2X7 receptors [26]. As expected, all microglial cells responded to the application of ATP (100 μM) with a clear increase of $[Ca^{2+}]_i$ (Fig. 1c, f, g; Table 1). The ATP-induced $Ca^{2+}$ mobilization was dependent on $Ca^{2+}$ entry from the extracellular space but also from intracellular compartments, as indicated by the smaller $[Ca^{2+}]_i$ increase observed upon removal of external $Ca^{2+}$ (Fig. 1d, f, g; Table 1). Under these conditions, the $Ca^{2+}$ transients had a smaller amplitude and a visible $Ca^{2+}$ response was observed in a reduced percentage of cells (65.2%; Fig. 1f), likely because the signals were close to the detection limit of the essay. Thapsigargin, a selective blocker of endoplasmic reticulum $Ca^{2+}$ ATPases [30], evoked small-amplitude $Ca^{2+}$ transients in a small percentage of cells (Table 1), confirming that in our preparation, the amount of $Ca^{2+}$ releasable from intracellular compartments is limited. To simulate the effects of an inflammatory stimulus, cells were preincubated with LPS for 48 h [22, 23]. Under these conditions, ATP-evoked $Ca^{2+}$ transients exhibited similar amplitudes (Fig. 1e, g) but faster kinetics than in unstimulated cells: both rise time and half decay time were significantly shorter than in untreated cells (Fig. 1e; Table 1).

The study of the $Ca^{2+}$-dependent regulation of ionic conductances in resting and LPS-treated human microglia strictly relies on good preservation of diffusible cytoplasm factors. Thus, whole-cell transmembrane current recordings were performed in the perforated patch-clamp configuration, avoiding cell dialysis [31]. A direct comparison showed that in the presence of high $[Ca^{2+}]_i$

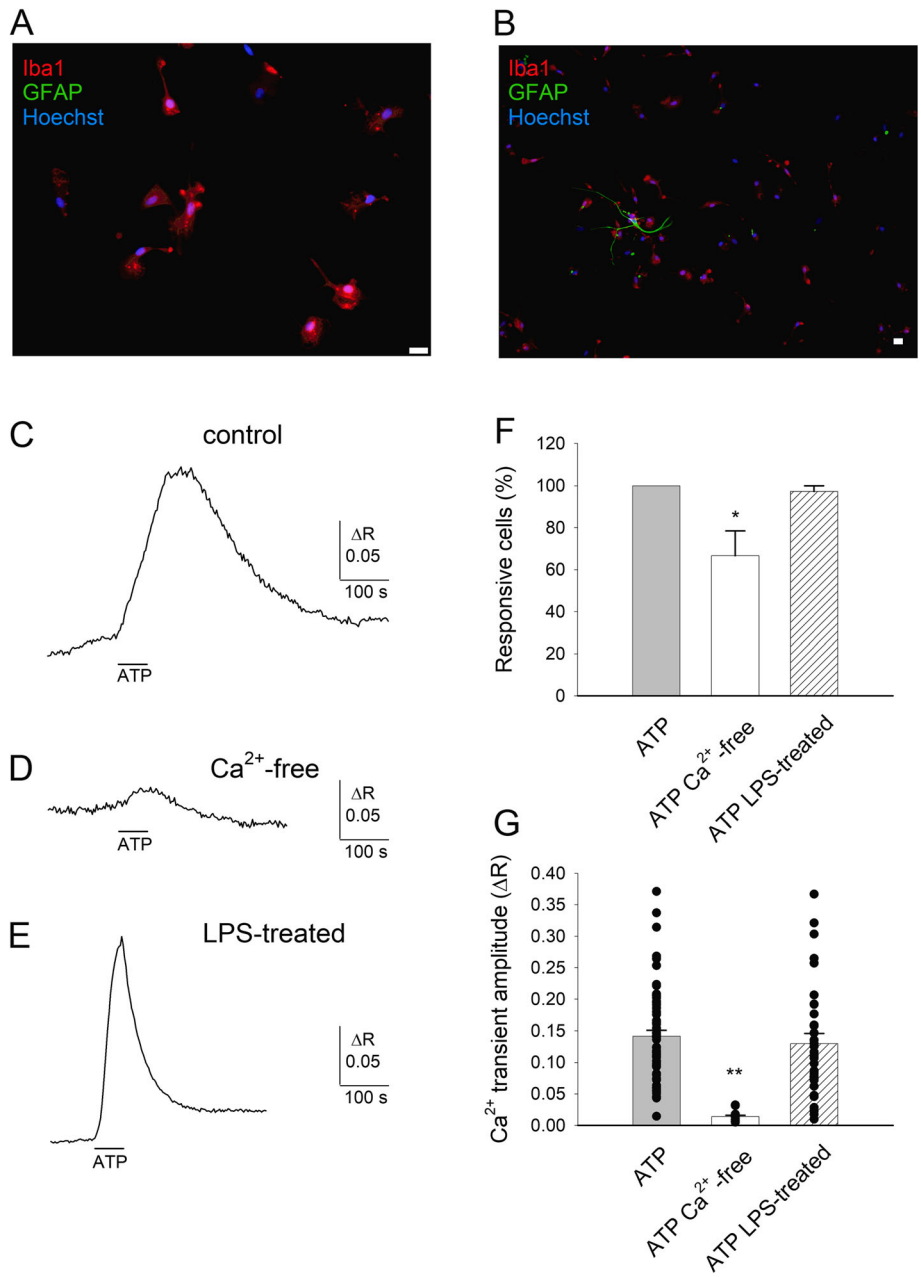


**Fig. 1** Extracellular ATP evokes $Ca^{2+}$ entry in highly pure primary cultures of human microglia. **a**, **b** Representative immunofluorescence images of primary cultures of human microglial cells (patient #12) marked with Iba1 and GFAP antibody (red and green, respectively) and nuclei marked with Hoechst 33258 (blue). Horizontal bar = 20 μm. Please note in **b** the presence of a single astrocyte. **c** Typical time-course of $[Ca^{2+}]_i$ changes elicited by ATP application (100 μM, 1 min, horizontal line) in a single human microglial cell (#9). **d** Typical time-course of $[Ca^{2+}]_i$ changes elicited by ATP application in the absence of external $Ca^{2+}$ (10 min preincubation; #10). **e** Typical time-course of $[Ca^{2+}]_i$ changes elicited by ATP application in a human microglial cell pretreated with LPS for 48 h (#12). **f** Histogram representing the percentage of microglial cells responding to ATP in control conditions (62 out 62 cells, 16 optical fields, #9), in $Ca^{2+}$-free medium (15 out 23 cells, 4 optical fields, #10; one asterisk denotes significantly different from control, $p$=0.023) or after LPS treatment (41 out 42 cells, 6 optical fields, #12). **g** Histogram representing the mean amplitude of ATP-induced $Ca^{2+}$ elevations, same cells as **c**, **d**, and **e**. Two asterisks denote significantly different from both other values, $p$<0.001. Black circles represent individual values

(1 μM) the current amplitudes recorded from dialyzed cells are much smaller than those recorded from intact cells with high $[Ca^{2+}]_i$ and are not significantly different from intact cells at rest (Fig. 2), confirming that the wash-out of intracellular factors, likely channel-activating $Ca^{2+}$-binding molecules, prevents a complete

**Table 1** Properties of $Ca^{2+}$ transients evoked in human microglial cells under different experimental conditions

| Stimulus | Resp. cells (%) | Basal (R) | Peak (R) | ΔR | $T_{0\text{-}100}$ (s) | $T_{100\text{-}50}$ (s) [n] |
|---|---|---|---|---|---|---|
| ATP | 100 (62/62) | 0.22±0.01 | 0.36±0.02 | 0.142±0.002 | 114±8 | 419±24 [27] |
| ATP (LPS) | 97.6 (41/42) | 0.219±0.007 | 0.35±0.02 | 0.13±0.02 | 67±6 | 353±24 [28] |
| ATP $Ca^{2+}$-free | 65.2 (15/23) | 0.177±0.007 | 0.191±0.008 | 0.014±0.004 | 336±29 | Nd [15] |
| GSK 1702934A | 61.6 (74/120) | 0.42±0.01 | 0.48±0.02 | 0.059±0.004 | 42±3 | 441±19 [29] |
| Thapsigargin | 28.4 (19/67) | 0.33±0.03 | 0.37±0.04 | 0.039±0.004 | 47±6 | 307±34 [5] |

Amplitude and kinetic parameters of evoked $Ca^{2+}$ transients were measured on a subset [n] of total responsive cells, in which it was possible to resolve the peak and the recovery of the $Ca^{2+}$ signal. Data were obtained from 3, 2, 3, 2, and 2 different patients for ATP, ATP in LPS-treated cells, ATP in $Ca^{2+}$-free, GSK 1702934A, and thapsigargin, respectively

current potentiation in response to $[Ca^{2+}]_i$ increase [15]. Under perforated patch conditions, during a stimulation protocol consisting of voltage ramps from −120 mV to +40 mV, applied every 2 s, the administration of ATP (100 μM) to human microglia induces a clear increase of the transmembrane current, as exemplified in Fig. 3a. Quantified at a membrane potential of −20 mV, this current potentiation was transient (Fig. 3b) and was completely abolished when $[Ca^{2+}]_i$ increase was prevented by removing external $Ca^{2+}$ and loading cells with the $Ca^{2+}$ chelator BAPTA-AM (20 μM, Fig. 3c, d). Following ATP application, the current density measured at −20 mV changed from a mean basal value of 0.9±0.2 pA/pF to a mean peak value of 4.8±1.5 pA/pF (Fig. 3g; $n$=13). In the absence of external $Ca^{2+}$ (Fig. 3e) or in cells preincubated with BAPTA-AM (Fig. 3f), the mean basal current density was reduced, as expected, to 0.6±0.1 pA/pF and 0.33±0.09 pA/pF (Fig. 3g; $n$=9 and $n$=5), respectively, with an ATP-induced effect that was significant only in $Ca^{2+}$-free conditions (1.1±0.2 pA/pF). In $Ca^{2+}$-free plus BAPTA conditions, the measured current density did not change from the basal value of 0.2±0.1 pA/pF. These results indicate that the ATP-mediated modulation of human microglial transmembrane currents depends on the ability of the cells to mobilize intracellular $Ca^{2+}$.

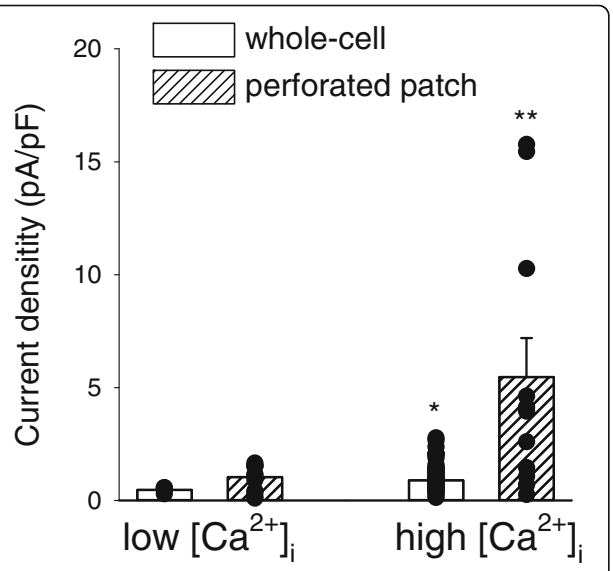


**Fig. 2** Intracellular dialysis limits the $Ca^{2+}$-induced potentiation of the whole-cell transmembrane currents recorded from human microglia. Histogram representing the mean whole-cell current densities recorded from human microglial cells in unstimulated conditions or in high $[Ca^{2+}]_i$ conditions, as indicated, with or without internal dialysis (white or hatched bars, respectively). High $[Ca^{2+}]_i$ condition was obtained by using a controlled intracellular solution containing 1 μM free $Ca^{2+}$. Black circles represent individual cells. High $[Ca^{2+}]_i$ values significantly higher than respective low $[Ca^{2+}]_i$ values. ANOVA, *$p$=0.023; **$p$<0.001. Number of cells, from left to right, 4 (patient #12), 13 (6 cells from #3, 5 from #9, and 2 from #12), 51 (9 cells from patient #1, 17 from #2, 6 from #5, and 19 from #13), 13 (6 cells from #3, 5 from #9, and 2 from #12), respectively

To dissect the molecular components of the $Ca^{2+}$-dependent currents, we first blocked the $K_{Ca}3.1$ channels, which were previously reported to constitute the major $K^+$ conductance in microglia from epileptic patients [2]. The selective $K_{Ca}3.1$ blocker TRAM-34 significantly reduced the mean peak value of the ATP-induced current potentiation (Fig. 4a, b), but did not completely abolish it. In the presence of TRAM-34, ATP potentiated the mean current density from 0.7±0.2 pA/pF to 1.6±0.3 pA/pF (Fig. 4d; $n$=10; $p$<0.001). The removal of external $Cl^-$ in the presence of TRAM-34 further lowered the ATP-evoked potentiation (Fig. 4c), which however was still significant: from 0.5±0.3 pA/pF to 1.0±0.5 pA/pF (Fig. 4d; $n$=7; $p$=0.031). This finding confirms the presence of a $Ca^{2+}$-dependent $Cl^-$ conductance, previously described in mice [28] also in human microglia. In contrast to what we observed with ATP-induced $Ca^{2+}$ mobilization, the treatment of microglial cells with LPS for 48 h completely abolished the ATP-mediated current potentiation (Fig. 5a). This result, unexpected based on previous studies [19], indicated a functional uncoupling between $[Ca^{2+}]_i$ increase and current potentiation and led us to analyze the functional expression of $K_{Ca}3.1$ channels upon LPS treatment. Towards this goal, we applied the selective $K_{Ca}3.1$ channel activator NS309 (500 nM) to microglial cells: in unstimulated control cells, NS309 produced a transient fivefold increase in the current measured at −20 mV (Fig. 5b, current density from 0.98±0.02 to 5.1±0.1 pA/pF; $n$=7). This effect was

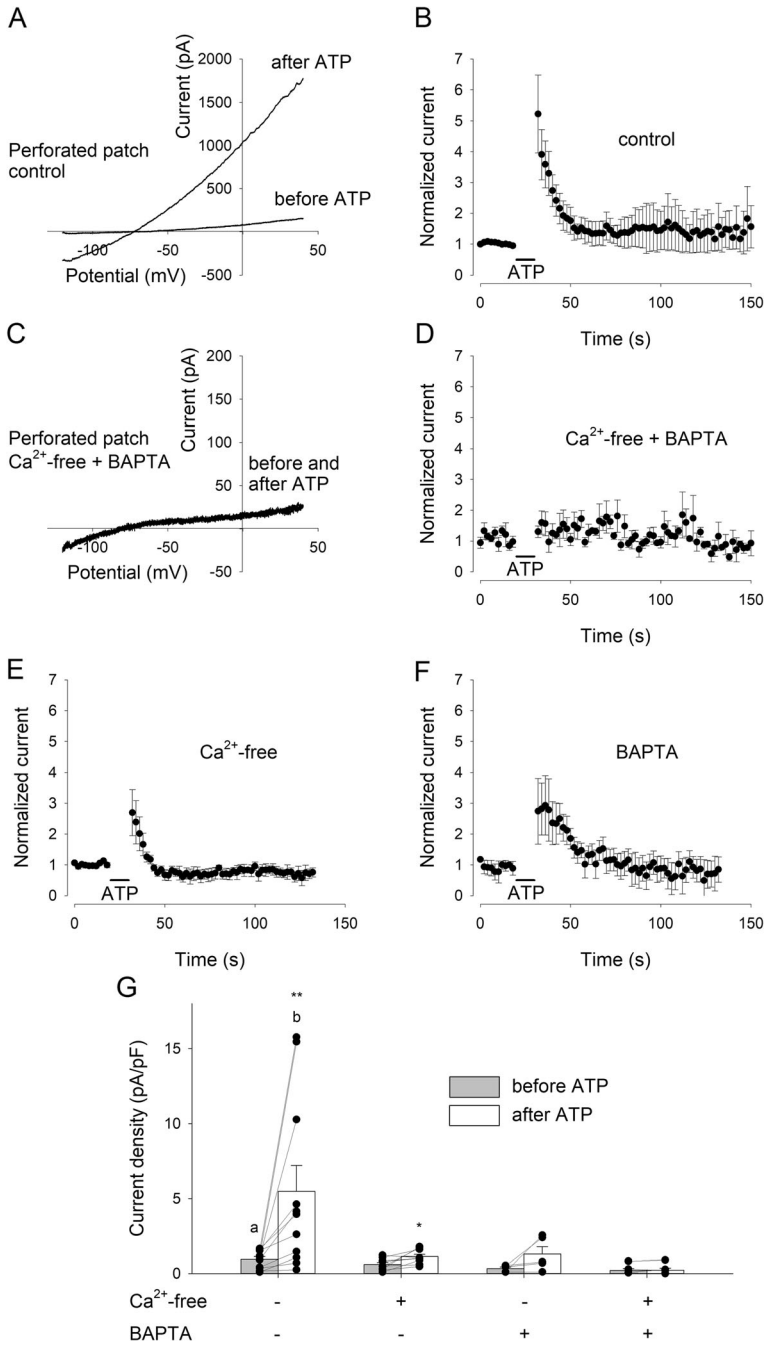


**Fig. 3** (See legend on next page.)

(See figure on previous page.)
**Fig. 3** The transient ATP-induced potentiation of whole-cell currents in human microglia depends on the $[Ca^{2+}]_i$ increase. **a** Typical I-V relation obtained by applying a single voltage ramp (from −120 mV to +40 mV, 200 ms) before and after the administration of ATP (100 μM, 10 s), on an representative human microglial cell (patient #3) out of the 11 cells recorded in the same conditions. Whole-cell currents were recorded in the voltage-clamp configuration using the perforated patch technique, to avoid cell dialysis. Please note the strong increase in the outward current after ATP. **b** Time course of the mean current amplitude measured at −20 mV in control conditions, averaged from 11 cells (6 from #3 and 5 from #9). Voltage ramps were applied every 2 s. Current amplitudes were normalized to the value averaged from the 5 currents preceding ATP administration. **c** Typical I-V relation obtained by applying a single voltage ramp before and after the administration of ATP, on a representative cell (#7) out of the 6 cells recorded in the same conditions. **d** Time course of the mean current amplitude measured at −20 mV in the absence of external $Ca^{2+}$ in cells preincubated with the $Ca^{2+}$ chelator BAPTA-AM (20 μM), averaged from 6 cells (#7). Please note that ATP-induced current potentiation is abolished if $[Ca^{2+}]_i$ increase is prevented. **e** Time course of the mean current amplitude measured at −20 mV in the absence of external $Ca^{2+}$, averaged from 9 cells (#10). **f** Time course of the mean current amplitude measured at −20 mV in cells preincubated with the $Ca^{2+}$ chelator BAPTA-AM (20 μM), averaged from 5 cells (#4). **g** Histogram representing the mean current density measured at −20 mV immediately before (gray) and after (white) the ATP administration, in different experimental conditions, as indicated. Please note that in the absence of extracellular $Ca^{2+}$ cells preincubated with BAPTA-AM shows a reduction of basal current density along with the complete lack of ATP-induced current potentiation. The numbers of recorded cells for control (left bars), $Ca^{2+}$-free, only BAPTA, and $Ca^{2+}$-free + BAPTA experiments (right bars) were 13 (6 from #3, 5 from #9 and 2 from #12), 9 (#10), 5 (#4), and 6 (#7), respectively. Two asterisks denote significantly higher than before ATP, $p<0.001$. *$p=0.025$. **a** Mean basal value in control condition is significantly higher than in BAPTA ($p=0.033$) and in $Ca^{2+}$-free + BAPTA ($p=0.007$). **b** Mean peak value in control condition is significantly higher than in $Ca^{2+}$-free ($p=0.020$), in BAPTA ($p=0.025$), and in $Ca^{2+}$-free + BAPTA ($p=0.006$)

significantly inhibited in LPS-treated cells, but not abolished (Fig. 5c, current density from 0.98±0.09 to 1.9±0.9 pA/pF; $n=5$). LPS treatment similarly decreases both the ATP- and NS309-mediated current potentiation (Fig. 5d), strongly suggesting that LPS incubation, in our conditions, causes a reduction of $K_{Ca}3.1$ function. A direct comparison shows a good correlation between the ATP-evoked mean current potentiation and mean $Ca^{2+}$ transient amplitude, lacking in LPS-treated human microglia (Fig. 6).

To verify whether the mechanism linking $Ca^{2+}$ mobilization and current modulation can be activated by other cellular pathways, we aimed to elicit intracellular $Ca^{2+}$ transients independently from ATP signaling. We, therefore, applied cholinergic agonists previously described to increase intracellular $Ca^{2+}$ in microglia (acetylcholine 100 μM or nicotine 5 μM [12, 32]), but in our hands, the cholinergic stimulation was never able to elicit a $Ca^{2+}$ signal or exert any effect on transmembrane currents (not shown). We then focused on store-operated $Ca^{2+}$ entry, a TRPC-dependent mechanism described in microglia [33]. We applied the selective TRPC3/6 channel activator GSK 1702934 (3 μM) to microglia and measured the $[Ca^{2+}]_i$ changes as well as the current modulation. This molecule evoked $Ca^{2+}$ transients (Fig. S1A) and caused small but significant current potentiation (Fig. S1B), confirming that $Ca^{2+}$ mobilized independently from purinergic signaling can affect microglial conductances.

## Discussion

Neuroinflammation alters the physiological function of the CNS by modifying the activity of both glia and neurons and the molecular pattern of the extracellular milieu, with significant variation of several mediators such as cytokines, chemokines, and neurotransmitters. Neuroinflammation is a key factor in epileptogenesis [34, 35]. In particular, an inflammatory phenotype of microglial cells has been linked to neurotoxic processes associated with epileptic seizures [1] as well as with epileptogenesis [36]. Microglia are deeply involved in epileptic processes (for review see [1, 37]). In mice, microglia depletion enhances seizure severity and neuronal damage [38], while phenotypic microglia alterations due to elevated mTOR signaling lead to reduced synapse density, moderate neuronal degeneration, and astrocyte proliferation, resulting in severe spontaneous recurrent seizures [39]. Furthermore, aberrant microglia-dependent synaptic pruning in the epileptic brain causes synaptic excitatory/inhibitory imbalance, promoting the progression of epilepsy [40].

Our results on primary microglia from the human epileptic temporal cortex contribute to better define the complex picture of microglial functions in epileptic patients. Even if, in general, studies on human CNS cells suffer from the scarcity of proper controls, they provide crucial information on the molecular and cellular pathways that could be targeted in human cells.

Specifically, our working hypothesis is that the acute response of microglia to extracellular ATP, a relevant mediator released during seizures [24], may be modulated to decrease the pathogenic pro-inflammatory potential of microglia. We confirmed that human microglia respond to extracellular ATP mobilizing intracellular $Ca^{2+}$ and increased $Ca^{2+}$ entry [15]. These cells express different purinergic receptors [4], such as the $Ca^{2+}$-permeable P2X7 and P2X4 ionotropic receptors and the $Ca^{2+}$-mobilizing P2Y metabotropic receptors [29, 41, 42]. P2Y1, P2Y12, and P2Y13 receptors participate in process movement in microglia from epileptic patients [29], and an increase of seizures has been observed in mice lacking the P2Y12 receptor [43]. However, ATP is

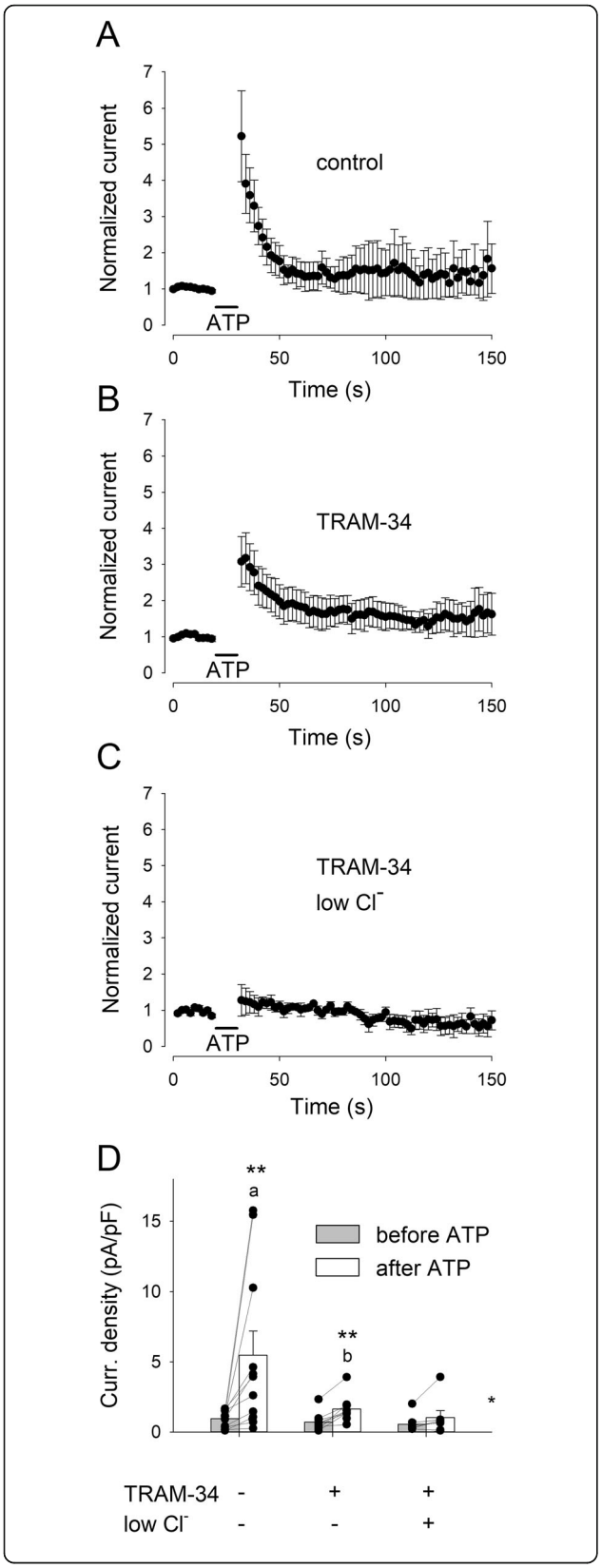


**Fig. 4** The ATP-induced current potentiation is due to $Ca^{2+}$-dependent $K^+$ and $Cl^-$ conductances. **a** Time course of the mean current amplitude measured at −20 mV in control conditions, averaged from 11 cells (6 from #3 and 5 from #9; same data of Fig. 3b). Voltage ramps were applied every 2 s. Current amplitudes were normalized to the value averaged from the 5 currents preceding ATP administration. **b** Time course of the mean current amplitude measured at −20 mV in the presence of TRAM-34 (1 μM), averaged from 10 cells (#3). **c** Time course of the mean current amplitude measured at −20 mV in the absence of external $Cl^-$ and in the presence of TRAM-34 (1 μM), averaged from 7 cells (#11). **d** Histogram representing the mean current density measured at −20 mV immediately before (gray) and after (white) the ATP administration, in different experimental conditions, as indicated. The numbers of recorded cells for control (left bars), only TRAM-34, and $Cl^-$-free + TRAM-34 (right bars) were 13 (6 from #3, 5 from #9, and 2 from #12), 10 (#3), and 7 (#11), respectively. Two asterisks denote significantly higher than before ATP, $p<0.001$. *$p=0.031$. **a** Mean peak value in control condition is significantly higher than in $Cl^-$-free + TRAM-34 ($p=0.016$). **b** Mean peak value in TRAM-34 is significantly higher than in $Cl^-$-free + TRAM-34 ($p=0.040$)

a weak partial agonist of both P2Y12 and P2Y13 receptors, which are fully activated by ADP [44]. Furthermore, we show that the block of endoplasmic reticulum $Ca^{2+}$ ATPases by thapsigargin evoked very small $Ca^{2+}$ mobilization. Pulled together, these observations suggest that in human microglia from epileptic patients the primary source of ATP-induced $[Ca^{2+}]_i$ increase is $Ca^{2+}$ entry through P2X ionotropic receptors. Upregulation of both P2X7 and P2X4 receptors has been observed in microglia following experimental seizures [45–47]. The ATP concentration used in the present study (100 μM), not able to activate the low-affinity P2X7 receptors ($EC_{50}$ in the millimolar range) [26], suggests that in our experiments ATP-induced $Ca^{2+}$ entry is primarily mediated by P2X4 receptors, confirming previous results in mouse microglia [42].

The transient increase of $[Ca^{2+}]_i$ is an essential step in microglial activation, modulating genetic transcription, motility, secretion, and other processes [11]. Furthermore, microglial calcium signaling is altered in awake mice following status epilepticus, indicating calcium as a key second messenger in microglia during epileptogenesis [27]. $Ca^{2+}$ activates several ion channels that affect microglial membrane potential [19]. Extracellular ATP potentiates the transmembrane currents measured in human microglia in a $Ca^{2+}$-dependent manner. However, this effect is completely abolished when $[Ca^{2+}]_i$ increases are inhibited by chelating $Ca^{2+}$. When we further dissected ionic components contributing to these $Ca^{2+}$-evoked currents, we found both a $Cl^-$ and a $K^+$ component. A $Ca^{2+}$-dependent $Cl^-$ conductance has been recently described in mouse hippocampus [28], but its physiological role needs to be studied in more detail in human cells. Here, we focused on the study of the $K^+$

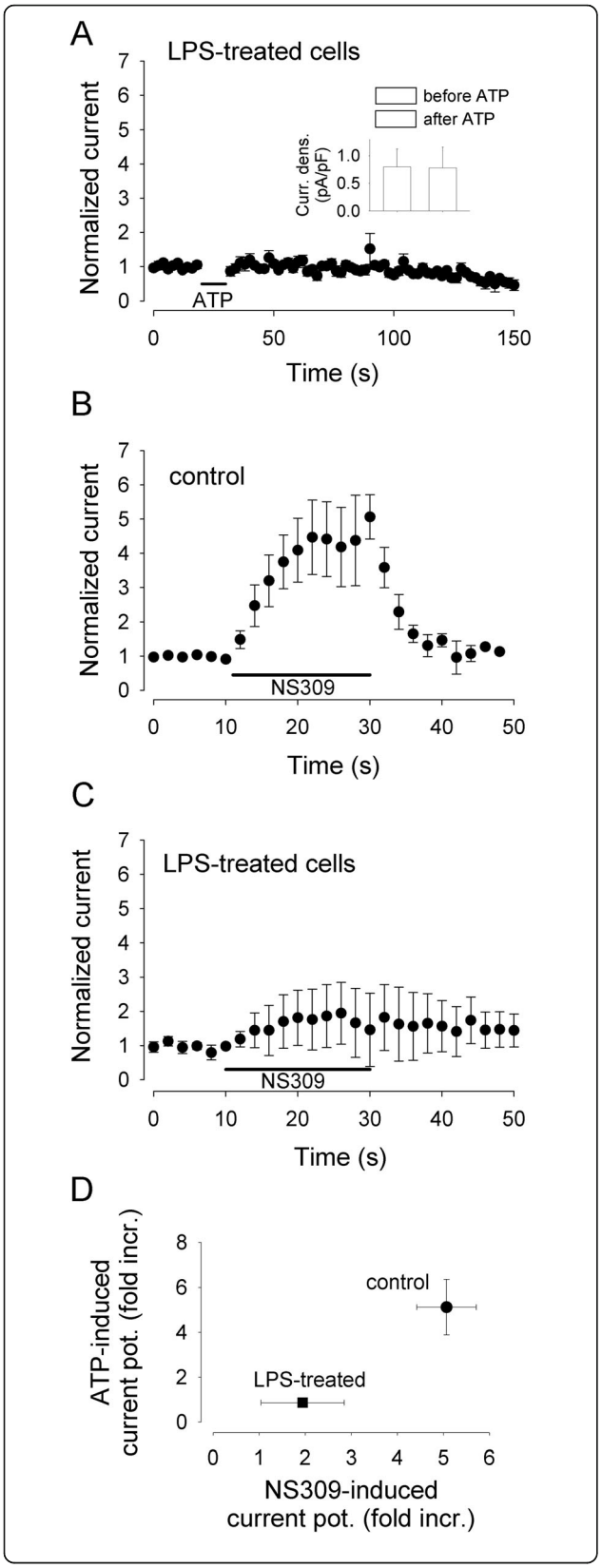


**Fig. 5** The ATP-induced current potentiation is downregulated in LPS-treated human microglia. **a** Time course of the mean current amplitude measured at −20 mV in control conditions, averaged from 5 cells (3 from #10 and 2 from #12) pre-treated with LPS (100 ng/ml for 48 h; LPS absent during the recording). Please note that LPS treatment completely abolished the ATP-induced current potentiation ($p$=0.027 when compared with control cells; $n$=5). **b** Time course of the mean current amplitude measured at −20 mV during the application of the selective $K_{Ca}3.1$ channel activator NS309 (500 nM, 20 s), averaged from 10 cells (2 from #5, 6 from #1, and 2 from #2). Voltage ramps applied every 2 s. Current amplitudes were normalized to the value averaged from the 5 currents preceding ATP administration. **c** Time course of the mean current amplitude during the application of NS309 on LPS-treated cells, averaged from 5 cells (#12). Please note that LPS treatment strongly reduced the NS309 effect. **d** Correlation plot linking the $Ca^{2+}$-mediated ATP-induced current potentiation to the $Ca^{2+}$-independent current potentiation induced by the selective $K_{Ca}3.1$ activator NS309. Data represent mean values ± standard error mean. Bidirectional errors are shown, sometimes not visible due to error amplitude smaller than symbol dimensions. Please note that LPS treatment reduces both types of modulation, indicating a reduction in the functional expression of $K_{Ca}3.1$ as the cause of the lack of $Ca^{2+}$-mediated current potentiation observed in LPS-treated cells

component of the $Ca^{2+}$ dependent conductance. Adult human microglia express different $K^+$ channels [19]. Our results confirm that the main channel responsible for the $Ca^{2+}$-induced $K^+$ current is $K_{Ca}3.1$ [19], as clearly established by the sensitivity of the current to TRAM-34 [48]. The intermediate-conductance $K_{Ca}3.1$ channel

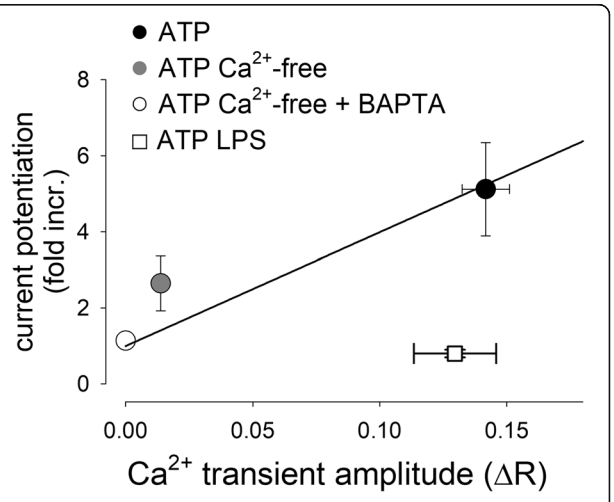


**Fig. 6** LPS-mediated microglia activation uncouples transmembrane currents from $[Ca^{2+}]_i$ by reducing the functional expression of $K_{Ca}3.1$. Correlation plot linking the current potentiation to the $Ca^{2+}$ transient amplitudes evoked by ATP in different experimental conditions. The solid line represents a linear regression constrained to pass through the point identified by the coordinates (0, 1). Please note that LPS treatment inhibits the current potentiation leaving unaltered the ability of ATP to increase $[Ca^{2+}]_i$. Data represent mean values ± standard error mean. Bidirectional errors are shown, sometimes not visible due to error amplitude smaller than symbol dimensions

mediates $Ca^{2+}$-induced hyperpolarization and is expressed by different cell types, including erythrocytes [49], leukocytes [50], vascular endothelium [51], bronchial epithelium [52], fibroblasts [53], and other cellular systems (for review see [54]). Consequently, $K_{Ca}3.1$ has been involved in many pathologies, including cardiovascular and respiratory disease [55, 56], diabetes [57], and tumor pathogenesis [58]. Several reports highlighted the pathological role of $K_{Ca}3.1$ in brain tumors, with a special focus on glioblastoma [59]. Many studies have identified $K_{Ca}3.1$ as a relevant therapeutical target, and several pharmacological tools have been developed [54], which could be helpful in different pathological contexts, including epilepsy [60].

The observed ATP-induced current potentiation was transient and was quantitatively correlated to $[Ca^{2+}]_i$ increase. The key role of $Ca^{2+}$ is confirmed by the fact that a small $[Ca^{2+}]_i$ increase due to a different stimulus, the activation of store-activated $Ca^{2+}$ entry mediated by TRPC3/6 [33], is still able to potentiate the microglial conductance. We also investigated the possibility that cholinergic stimulation could elicit $Ca^{2+}$ transients [32, 48], therefore, affecting microglial conductance, but in our experimental conditions, neither acetylcholine nor nicotine evoked a signal. These different results may arise from dissimilar conditions (species, pathology, age, culture conditions) and would require further investigation.

The activation of $K_{Ca}3.1$ by $Ca^{2+}$ is mediated by calmodulin [61], which is constitutively bound to the C-terminus of the channels [62] and can be modulated by other intracellular soluble factors, such as ATP or PKA [63–65]. For this reason, an intact cytoplasm is needed to study the modulation of $Ca^{2+}$ dependent conductances. Thus, the best experimental approach to analyze the function of microglial conductances is the perforated patch-clamp technique, avoiding intracellular dialysis [31]. To the best of our knowledge, our study is the first to apply perforated patch to adult human microglia. The complete or partial washout of diffusible factors during conventional whole-cell electrophysiological recording may affect the amplitudes, the kinetics, and the modulation properties of the recorded currents, leading to a profound alteration of the observed effects. These methodological considerations are particularly relevant when comparing microglial conductances in different conditions.

We used LPS treatment to investigate microglia response to ATP in an inflammatory environment. Detection of LPS in the brain is mainly carried out by Toll-like receptor 4, mostly expressed by microglia [66]. Selective microglial ablation in the dorsal hippocampus highlighted a neuroprotective role of microglia following a 24-h LPS treatment in the pilocarpine seizure model [67]. In our experimental conditions, LPS induced a complete block of ATP-mediated current potentiation in microglia, but did not affect basal $Ca^{2+}$ levels or inhibit ATP-induced $Ca^{2+}$ rise, indicating an uncoupling between $[Ca^{2+}]_i$ rise and current potentiation. Indeed, $K_{Ca}3.1$ function was strongly reduced in LPS-treated cells, as revealed using the selective activator NS309 [68]. The absence of the $Ca^{2+}$-evoked $K^+$ current, along with the associated hyperpolarization, led to a reduced ATP-evoked $Ca^{2+}$ entry, as shown by the faster $Ca^{2+}$-transient kinetics observed in LPS-treated microglia. This last finding confirms a crucial role for $Ca^{2+}$-activated $K^+$ channels in human microglia, i.e., sustaining hyperpolarization to prolong $Ca^{2+}$ entry [13]. The observation that LPS-treated microglial cells have a strongly reduced $K_{Ca}3.1$ function is in contrast to a previous study, showing that LPS treatment did not change the $K_{Ca}3.1$-mediated current in human microglia isolated from epileptic patients [3], in line with recent data showing a non-significant reduction of $K_{Ca}3.1$ gene expression in microglia from LPS-injected mice [69]. We posit that this discrepancy could be explained by the different experimental settings, perforated patch vs. whole-cell configuration: if LPS treatment reduced the $K_{Ca}3.1$ open probability through cytoplasmic diffusible factors, the resulting block of the $Ca^{2+}$-mediated current potentiation would not be detectable in conventional whole-cell recording conditions where diffusible factors and second messengers have been dialyzed out. Microglia, in response to pro-inflammatory molecules such as LPS, depending on the duration and/or concentration of stimulus [70], may produce either more pro-inflammatory or anti-inflammatory (e.g., IL-4 or IL-10) molecules [71]. In turn, these molecules could promote different phosphorylation pathways involved in the modulation of the $K_{Ca}3.1$ channel. An inhibitory effect of PKA on the human $K_{Ca}3.1$ channel was recently shown to be due to channel phosphorylation on S334, with the consequent reduction of the CAM binding affinity for the channel [41, 65]. By contrast, $K_{Ca}3.1$ channels are positively modulated by phosphorylation of H358 by nucleoside diphosphate kinase B [72].

What is the role of the ATP-evoked $Ca^{2+}$-dependent modulation of human microglial $K_{Ca}3.1$ channel in the context of epilepsy? Several reports indicated that the blockade of $K_{Ca}3.1$ could represent a candidate approach for epilepsy treatment [60, 73], due to its ability to impair sustained $Ca^{2+}$ entry in microglia during elevated neuronal activity and by shifting the phenotype of microglia towards an anti-inflammatory neuroprotective status [74, 75]. However, in a kindling model of temporal lobe epilepsy, $K_{Ca}3.1$ blockade did not prevent seizures and even exacerbated pathology-related neuronal damage [20]. Besides, in a model of chronic epilepsy, a

$Ca^{2+}$-sensitive $K_{Ca}3.1$-mediated component of the slow afterhyperpolarization of rat hippocampal pyramidal neurons has been reported to be downregulated by PKA [76]. Thus, future studies will be necessary to determine the role of $K_{Ca}3.1$ activity in the context of epilepsy, also considering that different experimental models may underlay different microglial phenotypes.

## Conclusion

Our data confirm a crucial role of $K_{Ca}3.1$ channel activity in microglial function in humans, linking ATP-induced $Ca^{2+}$ signals to conductance changes, in a cellular process modulated by inflammatory stimuli. Future experiments will reveal whether microglial KCa3.1 could be a target to decrease the inflammatory mechanisms triggered by purinergic signals during epilepsy.

## Supplementary Information

The online version contains supplementary material available at https://doi.org/10.1186/s12974-021-02096-0.

**Additional file 1: Figure S1.** The activation of TRPC3/6 channels increases $[Ca^{2+}]_i$ and potentiates the transmembrane currents in human microglia. **Table S1.** Patients included in the study.

### Abbreviations

ANOVA: Analysis of variance; ATP: Adenosine three phosphate; $[Ca^{2+}]_i$: Free calcium concentration; CNS: Central nervous system; cGMP: Cyclic guanosine monophosphate; GFAP: Glial fibrillary acidic protein; Iba1: Ionized calcium-binding adapter molecule 1; IL-4, IL-10: Interleukin type 4, 10; $K_{Ca}3.1$: Calcium-modulated potassium channel type 3.1; LPS: Lipopolysaccharide; PKA: Protein kinase type A; P2Y: Purinergic G protein-coupled receptors family; P2X4: Purinergic ionotropic receptor type 4; P2X7: Purinergic ionotropic receptor type 7; ROS: Reactive oxygen species; TRPC3/6: Transient receptor potential cation channels type 3/6

### Acknowledgements

We wish to thank Mrs. Annalisa Pagliuca for technical help.

### Authors' contributions

CL and SF designed the study. NPP, GC, and KM performed all the experiments. NPP and SF analyzed the results. AM, SC, and GDG selected epileptic patients. RM and VE performed neurosurgeries. NPP, KM, CL, HW, and SF wrote the manuscript. All authors reviewed and approved the final version of the manuscript.

### Funding

This study was supported by the Ricerca Corrente fund of the Italian Ministry of Health.

### Availability of data and materials

The datasets used and/or analyzed during the current study are available from the corresponding author on reasonable request.

### Ethics approval and consent to participate

Informed consent (MOD-D-SAN-95) was obtained from each patient to use part of the surgically resected material for experiments and the IRCCS Neuromed ethics committee approved the selection processes and procedures (approval number 5/2019).

### Consent for publication

Not applicable.

### Competing interests

The authors declare that they have no competing interests.

### Author details

[1]IRCCS Neuromed, Pozzilli, IS, Italy. [2]Department of Human Neurosciences, Sapienza Rome University, Rome, Italy. [3]Department of Pharmacology, University of California, Davis, CA, USA. [4]Department of Physiology and Pharmacology "V. Erspamer", Sapienza Rome University, Rome, Italy.

Received: 15 September 2020 Accepted: 2 February 2021
Published online: 15 February 2021

### References

1. Hiragi, T., Y. Ikegaya, and R. Koyama, Microglia after seizures and in epilepsy. Cells, 2018.7(4):26.
2. Streit WJ, et al. Role of microglia in the central nervous system's immune response. Neurol Res. 2005;27(7):685–91.
3. Whitelaw BS. Microglia-mediated synaptic elimination in neuronal development and disease. J Neurophysiol. 2018;119(1):1–4.
4. Prinz M, Jung S, Priller J. Microglia biology: one century of evolving concepts. Cell. 2019;179(2):292–311.
5. Hanisch UK. Microglia as a source and target of cytokines. Glia. 2002;40(2):140–55.
6. Morara S, Colangelo AM, Provini L. Microglia-induced maladaptive plasticity can be modulated by neuropeptides in vivo. Neural Plasticity. 2015;2015:135342.
7. Liu H, Leak RK, Hu XM. Neurotransmitter receptors on microglia. Stroke Vasc Neurol. 2016;1(2):52–8.
8. Calovi S, Mut-Arbona P, Sperlagh B. Microglia and the purinergic signaling system. Neuroscience. 2019;405:137–47.
9. Rassendren F, Audinat E. Purinergic signaling in epilepsy. J Neurosci Res. 2016;94(9):781–93.
10. McLarnon JG, et al. Perturbations in calcium-mediated signal transduction in microglia from Alzheimer's disease patients. J Neurosci Res. 2005;81(3):426–35.
11. Kettenmann H, et al. Physiology of microglia. Physiol Rev. 2011;91(2):461–553.
12. Sharma P, Ping L. Calcium ion influx in microglial cells: physiological and therapeutic significance. J Neurosci Res. 2014;92(4):409–23.
13. Stebbing MJ, Cottee JM, Rana I. The role of ion channels in microglial activation and proliferation - a complex interplay between ligand-gated ion channels, K+ channels, and intracellular Ca2+. Front Immunol. 2015;6:497.
14. Izquierdo P, Attwell D, Madry C. Ion channels and receptors as determinants of microglial function. Trends Neurosci. 2019;42(4):278–92.
15. Ferreira R, Wong R, Schlichter LC. KCa3:1/IK1 channel regulation by cGMP-dependent protein kinase (PKG) via reactive oxygen species and CaMKII in microglia: an immune modulating feedback system? Front Immunol. 2015;6:153.
16. Wu LJ, Vadakkan KI, Zhuo M. ATP-induced chemotaxis of microglial processes requires P2Y receptor-activated initiation of outward potassium currents. Glia. 2007;55(8):810–21.
17. Kittl M, et al. A swelling-activated chloride current in microglial cells is suppressed by Epac and facilitated by PKA - impact on phagocytosis. Cell Physiol Biochem. 2019;52(5):951–69.
18. Ishii TM, et al. A human intermediate conductance calcium-activated potassium channel. Proc Natl Acad Sci U S A. 1997;94(21):11651–6.
19. Blomster LV, et al. Quantification of the functional expression of the Ca(2+)-activated K(+) channel KCa 3.1 on microglia from adult human neocortical tissue. Glia. 2016;64(12):2065–78.
20. Ongerth T, et al. Targeting of microglial K(ca)3.1 channels by TRAM-34 exacerbates hippocampal neurodegeneration and does not affect ictogenesis and epileptogenesis in chronic temporal lobe epilepsy models. Eur J Pharmacol. 2014;740:72–80.
21. Rustenhoven J, et al. Isolation of highly enriched primary human microglia for functional studies. Sci Rep. 2016;6:19371.
22. Duan L, et al. LPS-induced proNGF synthesis and release in the N9 and BV2 microglial cells: a new pathway underling microglial toxicity in neuroinflammation. Plos One, 2013.8(9):e73768.
23. Nguyen HM, et al. Differential Kv1.3, KCa3.1, and Kir2.1 expression in "classically" and "alternatively" activated microglia. Glia. 2017;65:106–21.

24. Beamer E, Conte G, Engel T. ATP release during seizures - a critical evaluation of the evidence. Brain Res Bull. 2019;151:65–73.
25. Wang X, et al. Activation of purinergic P2X receptors inhibits P2Y-mediated Ca2+ influx in human microglia. Cell Calcium. 2000;27(4):205–12.
26. Coddou C, et al. Activation and regulation of purinergic P2X receptor channels. Pharmacol Rev. 2011;63(3):641–83.
27. Umpierre AD, et al. Microglial calcium signaling is attuned to neuronal activity in awake mice. Elife. 2020;9:e56502.
28. Murana E, et al. ATP release during cell swelling activates a Ca(2+)-dependent Cl(-) current by autocrine mechanism in mouse hippocampal microglia. Sci Rep. 2017;7(1):4184.
29. Milior G, et al. Distinct P2Y receptors mediate extension and retraction of microglial processes in epileptic and peritumoral human tissue. J Neurosci. 2020;40(7):1373–88.
30. Lytton J, Westlin M, Hanley MR. Thapsigargin inhibits the sarcoplasmic or endoplasmic reticulum Ca-ATPase family of calcium pumps. J Biol Chem. 1991;266(26):17067–71.
31. Schilling T, Eder C. Patch clamp protocols to study ion channel activity in microglia. Methods Mol Biol. 2013;1041:163–82.
32. Zhang L, et al. Cholinergic agonists increase intracellular Ca2+ in cultured human microglia. Neurosci Lett. 1998;255(1):33–6.
33. Ohana L, et al. The Ca2+ release-activated Ca2+ current (I(CRAC)) mediates store-operated Ca2+ entry in rat microglia. Channels (Austin). 2009;3(2):129–39.
34. Mahfoz AM, Shahzad N. Neuroinflammation impact in epileptogenesis and new treatment strategy. Behav Pharmacol. 2019;30(8):661–75.
35. Vezzani A, Balosso S, Ravizza T. Neuroinflammatory pathways as treatment targets and biomarkers in epilepsy. Nat Rev Neurol. 2019;15(8):459–72.
36. Alyu F, Dikmen M. Inflammatory aspects of epileptogenesis: contribution of molecular inflammatory mechanisms. Acta Neuropsychiatr. 2017;29(1):1–16.
37. Eyo UB, Murugan M, Wu LJ. Microglia-neuron communication in epilepsy. Glia. 2017;65:5–18.
38. Liu M, et al. Microglia depletion exacerbates acute seizures and hippocampal neuronal degeneration in mouse models of epilepsy. Am J Physiol Cell Physiol. 2020;319:C605–10.
39. Zhao X, et al. Noninflammatory changes of microglia are sufficient to cause epilepsy. Cell Rep. 2018;22:2080–93.
40. Andoh M, Ikegaya Y, Koyama R. Synaptic pruning by microglia in epilepsy. J Clin Med. 2019;8(12):2170.
41. Janks L, Sharma CVR, Egan TM. A central role for P2X7 receptors in human microglia. J Neuroinflammation. 2018;15(1):325.
42. Nguyen HM, et al. Biophysical basis for Kv1.3 regulation of membrane potential changes induced by P2X4-mediated calcium entry in microglia. Glia. 2020;68(11):2377–94.
43. Eyo UB, et al. Neuronal hyperactivity recruits microglial processes via neuronal NMDA receptors and microglial P2Y12 receptors after status epilepticus. J Neurosci. 2014;34(32):10528–40.
44. Bianco F, et al. Pathophysiological roles of extracellular nucleotides in glial cells: differential expression of purinergic receptors in resting and activated microglia. Brain Res Rev. 2005;48(2):144–56.
45. Rappold PM, Lynd-Balta E, Joseph SA. P2X7 receptor immunoreactive profile confined to resting and activated microglia in the epileptic brain. Brain Res. 2006;1089(1):171–8.
46. Avignone E, et al. Status epilepticus induces a particular microglial activation state characterized by enhanced purinergic signaling. J Neurosci. 2008;28(37):9133–44.
47. Ulmann L, et al. Involvement of P2X4 receptors in hippocampal microglial activation after status epilepticus. Glia. 2013;61(8):1306–19.
48. Wulff H, et al. Design of a potent and selective inhibitor of the intermediate-conductance Ca2+-activated K+ channel, IKCa1: a potential immunosuppressant. Proc Natl Acad Sci U S A. 2000;97(14):8151–6.
49. Gardos G. The function of calcium in the potassium permeability of human erythrocytes. Biochim Biophys Acta. 1958;30:653–4.
50. Cahalan MD, Chandy KG. The functional network of ion channels in T lymphocytes. Immunol Rev. 2009;231:59–87.
51. Si H, et al. Impaired endothelium-derived hyperpolarizing factor-mediated dilations and increased blood pressure in mice deficient of the intermediate-conductance $Ca^{2+}$-activated $K^+$ channel. Circ Res. 2006;99:537–44.
52. Arthur GK, et al. KCa3.1 K+ channel expression and function in human bronchial epithelial cells. PLoS One. 2015;10:e0145259.
53. Grgic I, et al. Renal fibrosis is attenuated by targeted disruption of KCa3.1 potassium channels. Proc Natl Acad Sci U S A. 2009;106:14518–23.
54. Brown BM, et al. Pharmacology of small- and intermediate-conductance calcium-activated potassium channels. Annu Rev Pharmacol Toxicol. 2020;60:219–40.
55. Roach KM, et al. The K+ channel KCa3.1 as a novel target for idiopathic pulmonary fibrosis. Plos One. 2013;8:e85244.
56. Köhler R, Oliván-Viguera A, Wulff H. Endothelial small- and intermediate-conductance K channels and endothelium-dependent hyperpolarization as drug targets in cardiovascular disease. Adv Pharmacol. 2016;77:65–104.
57. Huang C, Pollock CA, Chen XM. Role of the potassium channel KCa3.1 in diabetic nephropathy. Clin Sci. 2014;127:423–33.
58. Mohr CJ, et al. Cancer-associated intermediate conductance Ca(2+)-activated K+ channel K(Ca)3.1. Cancers. 2019;11:109.
59. D'Alessandro G, Limatola C, Catalano M. Functional roles of the Ca2+-activated K+ channel, KCa3.1, in brain tumors. Curr Neuropharmacol. 2018;16:636–43.
60. Christophersen P, Wulff H. Pharmacological gating modulation of small- and intermediate-conductance Ca(2+)-activated K(+) channels (KCa2.x and KCa3.1). Channels. 2015;9(6):336–43.
61. Fanger CM, et al. Calmodulin mediates calcium-dependent activation of the intermediate conductance KCa channel, IKCa1. J Biol Chem. 1999;274(9):5746–54.
62. Lee CH, MacKinnon R. Activation mechanism of a human SK-calmodulin channel complex elucidated by cryo-EM structures. Science. 2018;360(6388):508–13.
63. Gerlach AC, et al. ATP-dependent activation of the intermediate conductance, Ca2+-activated K+ channel, hIK1, is conferred by a C-terminal domain. J Biol Chem. 2001;276(24):10963–70.
64. Wong R, Schlichter LC. PKA reduces the rat and human KCa3.1 current, CaM binding, and Ca2+ signaling, which requires Ser332/334 in the CaM-binding C terminus. J Neurosci. 2014;34(40):13371–83.
65. Sforna L, et al. Structure, gating and basic functions of the Ca2+-activated K channel of intermediate conductance. Curr Neuropharmacol. 2018;16(5):608–17.
66. Zhang Y, et al. An RNA-sequencing transcriptome and splicing database of glia, neurons, and vascular cells of the cerebral cortex. J Neurosci. 2014;34:11929–47.
67. Mirrione MM, et al. Microglial ablation and lipopolysaccharide preconditioning affects pilocarpine-induced seizures in mice. Neurobiol Dis. 2010;39(1):85–97.
68. Strobaek D, et al. Activation of human IK and SK Ca2+ -activated K+ channels by NS309 (6,7-dichloro-1H-indole-2,3-dione 3-oxime). Biochim Biophys Acta. 2004;1665(1-2):1–5.
69. Srinivasan K, et al. Alzheimer's patient microglia exhibit enhanced aging and unique transcriptional activation. Cell Rep. 2020;31(13):107843.
70. Horvath RJ, et al. Differential migration, LPS-induced cytokine, chemokine, and NO expression in immortalized BV-2 and HAPI cell lines and primary microglial cultures. J Neurochem. 2008;107(2):557–69.
71. Lively S, Schlichter LC. Microglia responses to pro-inflammatory stimuli (LPS, IFN gamma plus TNF alpha) and reprogramming by resolving cytokines (IL-4, IL-10). Front Cell Neurosci. 2018;12:215.
72. Srivastava S, et al. Histidine phosphorylation of the potassium channel KCa3.1 by nucleoside diphosphate kinase B is required for activation of KCa3.1 and CD4 T cells. Mol Cell. 2006;24(5):665–75.
73. Wulff H, et al. Modulators of small- and intermediate-conductance calcium-activated potassium channels and their therapeutic indications. Curr Med Chem. 2007;14(13):1437–57.
74. Chen YJ, et al. The potassium channel KCa3.1 constitutes a pharmacological target for neuroinflammation associated with ischemia/reperfusion stroke. J Cereb Blood Flow Metab. 2016;36(12):2146–61.
75. Cocozza G, et al. Ca(2+)-activated K(+) channels modulate microglia affecting motor neuron survival in hSOD1(G93A) mice. Brain Behav Immun. 2018;73:584–95.
76. Tiwari MN, et al. Protein kinase A-mediated suppression of the slow afterhyperpolarizing KCa3.1 current in temporal lobe epilepsy. J Neurosci. 2019;39(50):9914–26.


## Publisher's Note

**Supplementary information**

*Figure S1. The activation of TRPC3/6 channels increases $[Ca^{2+}]_i$ and potentiates the transmembrane currents in human microglia.*

A, typical time-course of $[Ca^{2+}]_i$ changes elicited by application of GSK 1702934A, a selective agonist of TRPC3/6 channels (3 μM, 40 s, horizontal line) in a representative human microglial cell (patient #6). B, time course of the normalized mean current amplitude measured at -20 mV during GSK 1702934A application, averaged from 9 cells (2 from #6, 2 from #7 and 5 from #8). Voltage ramps were applied every 2s. Inset, histogram representing the mean current density at -20 mV before (grey) and at the end (white) of GSK 1702934A application. Black circles represent values from individual cells.

Table S1. Patients included in the study

| Patient | Sex | Age at epilepsy onset (years) | Age at surgery (years) | Surgery | Histopathology |
|---|---|---|---|---|---|
| #1 | F | 25 | 29 | L-ATL | HS |
| #2 | F | 1 | 21 | L-ATL | HS |
| #3 | M | 21 | 44 | R-ATL | HS |
| #4 | M | 2 | 41 | L-ETL | HS |
| #5 | F | 21 | 41 | R-ATL | normal |
| #6 | M | 14 | 23 | Lesionectomy + R-ATL | DNET |
| #7 | M | 20 | 46 | R-ATL | HS |
| #8 | M | 15 | 26 | L-ATL | normal |
| #9 | M | 19 | 26 | R-ETL | FCDII A |
| #10 | M | 8 | 27 | L-ATL | HS |
| #11 | M | 14 | 50 | L-ATL | HS |
| #12 | F | 15 | 29 | L-ATL | HS |
| #13 | M | 25 | 27 | L-ATL | HS+ gangliocytoma |

L: left, R: right, ETL: extended temporal lobectomy, ATL: anterior temporal lobectomy, HS: hippocampal sclerosis, DNET: Dysembryoplastic neuroepithelial tumour, FCD: focal cortical dysplasia.